Available online at www.sciencedirect.com
ScienceDirect
Karbala International Journal of Modern Science 1 (2015) 32–38
http://www.journals.elsevier.com/karbala-international-journal-of-modern-science/

Photoinduced oxidative transformation of diphenylamine on Al_2O_3 with enhancement by ZnO synergism

C. Karunakaran*, S. Karuthapandian [1], P. Vinayagamoorthy

Department of Chemistry, Annamalai University, Annamalainagar 608002, Tamilnadu, India

Received 10 April 2015; revised 6 June 2015; accepted 7 June 2015
Available online 30 August 2015

Abstract

Diphenylamine (DPA) in ethanol on the surface of Al_2O_3 undergoes light-induced oxidative transformation affording N-phenyl-*p*-benzoquinonimine (PBQ). The photoinduced transformation on Al_2O_3 enhances with [DPA], Al_2O_3-loading, airflow rate and photon flux. The formation of PBQ on Al_2O_3 is larger under UV-C light than under UV-A light. The Al_2O_3 surface does not lose it activity on reuse. The mechanism of photoinduced oxidative transformation of DPA on Al_2O_3 has been discussed with appropriate kinetic law. ZnO enhances the UV light-induced transformation of DPA on Al_2O_3 indicating synergism.

Keywords: Photooxidation; Insulator; Semiconductor; Synergism

1. Introduction

Reports on semiconductor-photocatalyzed selective organic oxidative transformations are many [1–6] but those mediated by insulator Al_2O_3 are rare [7–10]. Semiconductors on band gap-illumination generate electron–hole pairs which initiate the photocatalytic reactions. Al_2O_3 is a wide band gap (*ca.* 9 eV) dielectric material and provides only non-reactive surfaces – photoproduction of charge carriers with UV light is energetically unviable. However, it controls significantly the photochemical reactivity of adsorbed molecules through electronic interactions and facilitates Norrish type II photoreaction of alkyl aryl ketones [7]. In addition, calcination at high temperature creates active sites which enable photoreactions on Al_2O_3 surface; intrinsic surface-perturbed defects such as oxygen monovacancies (F^+ and F) and aggregated oxygen vacancies (F_2, F_2^+ and F_2^{2+}) lead to formation of active sites [11]. Here we report for the first time photoinduced oxidative transformation of diphenylamine on untreated Al_2O_3 which is reusable. Furthermore, the rate of conversion is comparable to that on semiconductor surface. Diphenylamine (DPA) is used in post-harvest treatment of apple and pear [12] and photosensitized oxidation of DPA has been reported; the photosensitizers employed include cyanoanthracenes [13] and benzophenone [14].

* Corresponding author. Tel.: +91 9443481590; fax: +91 4144238145.
E-mail address: karunakaranc@rediffmail.com (C. Karunakaran).
Peer review under responsibility of University of Kerbala.
[1] Present address: Department of Chemistry, VHNSN College, Virudhunagar 626001, Tamilnadu, India.

http://dx.doi.org/10.1016/j.kijoms.2015.06.003

The unsensitized photooxidation of DPA to N-phenyl-*p*-benzoquinonimine (PBQ) is slow [15]. The chemical transformation was studied in the absence and presence of Al_2O_3 to obtain the rate of PBQ formation on Al_2O_3. The oxidative transformation on Al_2O_3 surface was studied with UV light and with natural sunlight under different experimental conditions to deduce the kinetic model and to elucidate the reaction mechanism; about 5% of UV light in the natural sunlight itself brings in the phototransformation on A_2O_3. The light-induced conversion of DPA to PBQ on Al_2O_3 is enhanced on mixing semiconductor ZnO with Al_2O_3 and this enhancement is ascribed to synergistic effect.

2. Experimental

2.1. Materials and measurements

Al_2O_3 (Merck) and ZnO (Merck) were used as received and their specific surface areas, determined by Brunauer–Emmett–Teller (BET) method, are 10.6 and 12.2 $m^2\ g^{-1}$, respectively. The mean particle sizes (t) of Al_2O_3 and ZnO, obtained using the formula $t = 6/\rho S$, where ρ is the material density and S is the specific surface area, are 167 and 87 nm, respectively. The obtained powder X-ray diffractograms (XRD) show the alumina used as a blend of gamma and chi phases (γ:χ:52:48) and ZnO in hexagonal zincite lattice [16]. The mean crystallite sizes obtained from the XRD results agree with those deduced from BET surface area measurements. The UV–visible diffuse reflectance spectra (DRS) of the materials were obtained using a Shimadzu UV-2600 spectrophotometer with ISR-2600 integrating sphere attachment. The Kubelka–Munk plot provides the band gap of ZnO as 3.15 eV. Potassium tris(oxalato)ferrate(III), $K_3[Fe(C_2O_4)_3]\cdot 3H_2O$, was prepared by standard method [17]. DPA, analytical reagent (Merck) was used as received. Commercial ethanol was purified by distillation with calcium oxide.

2.2. UV light-induced transformation

The UV light-induced transformation on Al_2O_3 was carried out in a multilamp photoreactor fixed with eight 8 W mercury UV lamps (Sankyo Denki, Japan) of wavelength 365 nm. The lamps were shielded by highly polished anodized aluminum reflector. Four cooling fans fixed at the bottom of the reactor dissipate the heat produced. The reaction vessel was a borosilicate glass tube of 15-mm inner diameter and was placed at the center of the photoreactor. The UV light-induced reaction was also studied with a microphotoreactor equipped with a 6 W 254 nm low-pressure mercury lamp and a 6 W 365 nm mercury lamp. Quartz and borosilicate glass tubes were used as reaction vessels for 254 and 365 nm lamps, respectively. The light intensity (I) was measured by ferrioxalate actinometry. The volume of the reaction solution was always maintained as 25 mL in the multilamp photoreactor and 10 mL in the microphotoreactor. Air was bubbled through the solution and the airflow rate was measured by soap bubble method. The UV–visible spectra were recorded with a Hitachi U-2001 UV–visible spectrophotometer. The solution was diluted 5-times to decrease the absorbance to the Beer–Lambert law limit. The PBQ formed was estimated from its absorbance at 450 nm.

2.3. Sunlight-induced transformation

The sunlight-induced reaction on Al_2O_3 was carried out under clear sky in summer (March–July) at 11.30 am − 12.30 pm. The solar irradiance (W m^{-2}) was measured with a Global pyranometer, supplied by Industrial Meters, Bombay, India. The sunlight intensity (Einstein (E) $L^{-1}\ s^{-1}$) was also measured by ferrioxalate actinometry. The measured 440 W m^{-2} corresponds to 22 μE $L^{-1}\ s^{-1}$. Ethanolic solutions of DPA of desired concentration were prepared afresh and taken in wide cylindrical glass vessels of uniform diameter. The entire bottom of the vessel was covered with Al_2O_3 powder. Air was bubbled through a micropump without disturbing the catalyst bed. The volume of DPA solution was 25 mL and the loss of solvent due to evaporation was compensated periodically. PBQ formed was estimated spectrophotometrically.

3. Results and discussion

3.1. UV light-induced oxidative transformation on Al_2O_3

The UV light-induced oxidative transformation of DPA in ethanol on Al_2O_3 surface was carried out by bubbling air in a multilamp photoreactor fixed with UV lamps of wavelength 365 nm. The UV–visible spectra of the DPA solution, obtained at different illumination time show the formation of PBQ ($\lambda_{max} = 450$ nm). The time spectra are presented in Fig. 1. The illuminated solution is EPR silent revealing the absence of formation of diphenylnitroxide. In addition, thin layer chromatographic analysis shows formation of a single product. The illuminated DPA solution was evaporated

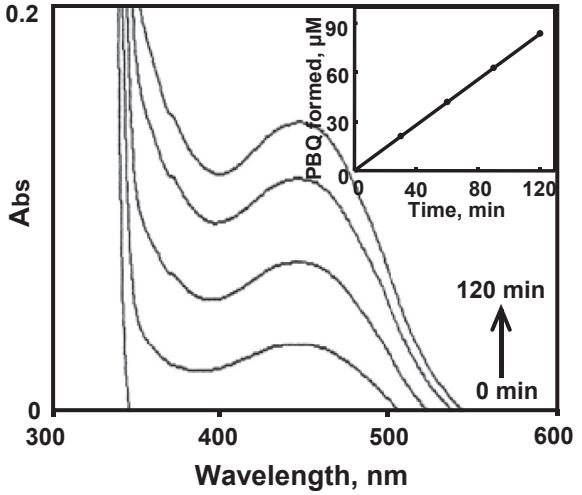

Fig. 1. UV light-induced PBQ formation with Al_2O_3 in ethanol: the UV–visible spectra of reaction solution (5-times diluted) at 0, 30, 60, 90 and 120 min (↑); [DPA] = 20 mM, Al_2O_3-loading = 1.0 g, airflow rate = 7.8 mL s^{-1}, I = 25.2 μE L^{-1} s^{-1}, volume of reaction solution = 25 mL; Inset: Linear increase of PBQ formed with illumination time.

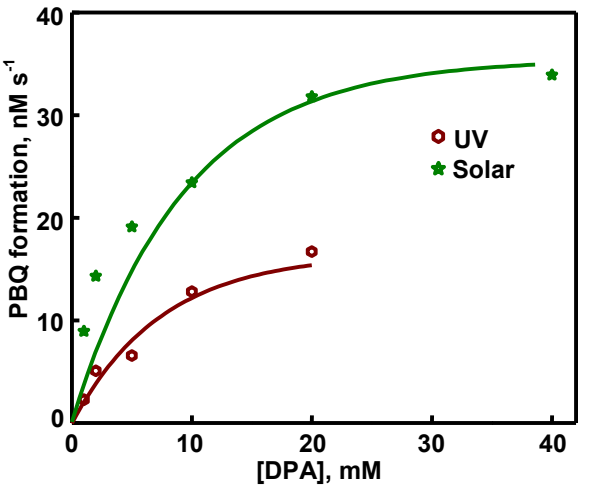

Fig. 2. Photoinduced PBQ formation on Al_2O_3 at different [DPA]; Al_2O_3-loading = 1.0 g, volume of reaction solution = 25 mL; UV: λ = 365 nm, I = 25.2 μE L^{-1} s^{-1}, airflow rate = 7.8 mL s^{-1}; Solar: bed area = 11.36 cm^2, airflow rate = 4.6 mL s^{-1}.

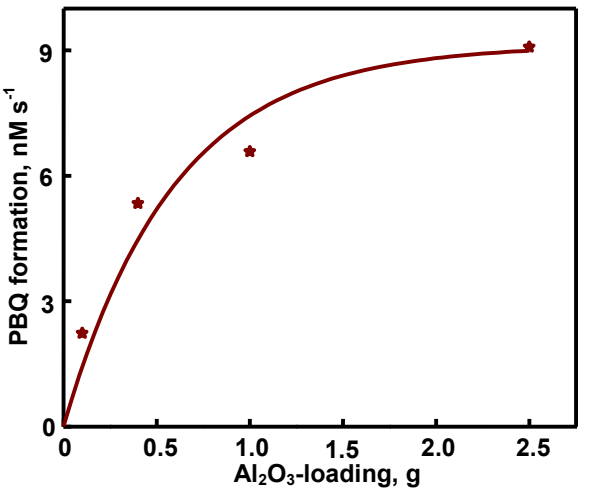

Fig. 3. Light-induced PBQ formation on Al_2O_3 at different Al_2O_3-loading; [PBQ] = 5.0 mM, airflow rate = 7.8 mL s^{-1}, λ = 365 nm, I = 25.2 μE L^{-1} s^{-1}, volume of reaction solution = 25 mL.

after the recovery of Al_2O_3 particles and the solid was dissolved in chloroform to develop the chromatogram on a silica gel G-coated plate employing benzene as eluent. The PBQ formed was estimated from its absorbance at 450 nm using the reported molar absorptivity [18,19]. The linear increase of [PBQ] with illumination time, as shown in Fig. 1 as inset, affords the PBQ formation rate and the rates are reproducible within ±6%. The direct photooxidation of DAP, the photoformation of PBQ in the absence of Al_2O_3, is slow [15] and the rate of PBQ formation on Al_2O_3 was obtained by determining the rates of PBQ formation in the presence and absence of Al_2O_3. Fig. 2 exhibits the enhancement of PBQ formation on Al_2O_3 with [DPA]. The observed enhancement conforms to the Langmuir–Hinshelwood kinetics with respect to [DPA]. The rate of surface reaction increases with loading of Al_2O_3 in the DPA solution and the rate attains a limit at high Al_2O_3-loading. Fig. 3 presents the results. Study of PBQ formation on Al_2O_3 as a function of airflow rates shows enhancement of the surface reaction by oxygen and the rate dependence on the airflow rate conforms to the Langmuir–Hinshelwood kinetic law. Fig. 4 displays the results. The PBQ formation on Al_2O_3 was also determined without bubbling air but the solution was not deoxygenated. The dissolved oxygen itself effects the photoinduced surface reaction. However, the reaction is slow. PBQ formation on Al_2O_3 was investigated at different intensities of illumination. The chemical transformation was carried out with two, four and eight lamps and the angles sustained by the adjacent lamps are 180°, 90° and 45°, respectively. Fig. 5 shows the dependence of the surface reaction rate on photon flux. PBQ is not formed in the absence of illumination. Study of the PBQ formation on Al_2O_3 under UV-A and UV-C light, employing a 6 W 365 nm mercury lamp (I = 18.1 μE L^{-1} s^{-1}) and a 6 W 254 nm low-pressure mercury lamp (I = 5.22 μE L^{-1} s^{-1}), separately in the microphotoreactor under identical conditions shows that

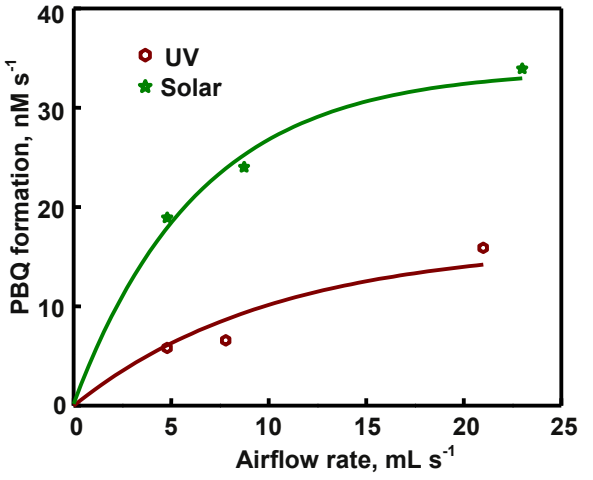

Fig. 4. Photoformation of PBQ on Al_2O_3 as a function of airflow rate; [DPA] = 5.0 mM, Al_2O_3-loading = 1.0 g, volume of reaction solution = 25 mL; UV: λ = 365 nm, I = 25.2 μE L^{-1} s^{-1}; Solar: bed area = 11.36 cm^2.

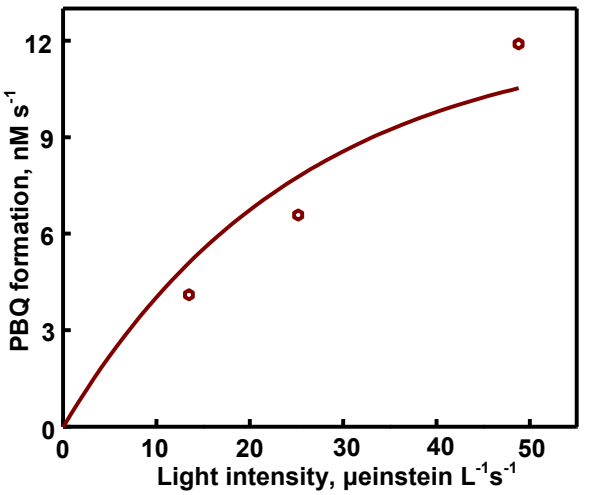

Fig. 5. Effect of photon flux on PBQ formation on Al_2O_3 surface; [DPA] = 5.0 mM, Al_2O_3-loading = 1.0 g, airflow rate = 7.8 mL s^{-1}, λ = 365 nm, volume of reaction solution = 25 mL.

UV-C light is more efficient than UV-A light in inducing the organic transformation on Al_2O_3. The PBQ formation with UV-A and UV-C light are 3.8 and 28.0 nM s^{-1}, respectively ([DPA] = 5.0 mM, Al_2O_3 suspended: 1.0 g, airflow rate = 7.8 mL s^{-1}). Al_2O_3 retains its activity on usage. Reuse of Al_2O_3 shows sustainable photoinduced PBQ formation. Singlet oxygen quencher azide ion (5 mM) does not suppress the PBQ formation revealing the absence of involvement of singlet oxygen in the photoinduced organic transformation on Al_2O_3. This is in line with the literature report; Fox and Chen [20] ruled out the possibility of singlet oxygen in the TiO_2-photocatalyzed olefin-to-carbonyl oxidative cleavage.

3.2. Sunlight-induced oxidative transformation on Al_2O_3

The oxidative transformation of DPA into BPQ on Al_2O_3 surface occurs under natural sunlight as well. The UV–visible spectrum of sun-shined DPA solution in ethanol, in the presence of Al_2O_3 and air, is similar to that with UV light (λ_{max} = 450 nm). Furthermore, the sun-shined solution is electron paramagnetic resonance (EPR) silent showing the absence of diphenylnitroxide. In addition, thin-layer chromatographic (TLC) analysis reveals formation of a single product. Measurement of the solar irradiance (W m^{-2}) shows fluctuation of sunlight intensity during the experiment even under clear sky. Hence, the solar experiments at different reaction conditions were performed in a set to maintain the quantum of sunlight incident on unit area the same. This makes possible comparison of the solar results. A pair of solar experiments carried out simultaneously under identical reaction conditions provides results within ±6% and this is so on different days. The effect of operational parameters on the solar-induced oxidative transformation was studied by carrying out the given set of experiments simultaneously and the results shown in each figure represent identical solar irradiance. The rate of PBQ formation was obtained by shining the DPA solution on Al_2O_3 bed for 60 min. The dependence of PBQ formation rate on [DPA] is displayed in Fig. 2. The observed increase of PBQ formation with [DPA] is characteristic of the Langmuir–Hinshelwood kinetic law. The double reciprocal plot of PBQ formation rate versus [DPA] is a straight line with a positive y-intercept (figure not presented), which confirms the Langmuir–Hinshelwood kinetic model. Fig. 4 presents the rate of PBQ formation on Al_2O_3 at different airflow rates. The observed enhancement of the PBQ formation by oxygen shows that the surface reaction conforms to Langmuir–Hinshelwood kinetics with respect to oxygen also. The double reciprocal plot of reaction rate versus airflow rate is linear with a finite y-intercept (figure not given). The PBQ formation on Al_2O_3 was studied without bubbling air but the solution was not deoxygenated. The dissolved oxygen is sufficient to effect the chemical transformation on Al_2O_3 during the experimental period. However, the transformation is slow. The PBQ formation on Al_2O_3 increases linearly with the apparent area of Al_2O_3-bed. Fig. 6 presents

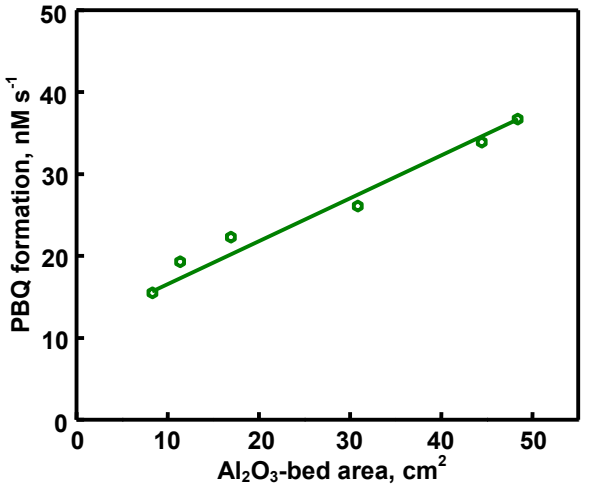

Fig. 6. Dependence of sunlight-induced PBQ formation rate on Al_2O_3-bed area; [DPA] = 5.0 mM, Al_2O_3 loading = 1.0 g, airflow rate = 4.6 mL s^{-1}, volume of reaction solution = 25 mL.

the results. The oxidative transformation does not take place in the absence of sunlight. Al_2O_3 does not lose its activity on usage. Reuse of Al_2O_3 shows sustainable activity.

3.3. Mechanism

The band gap of Al_2O_3 is large and pristine Al_2O_3 does not absorb significantly in the UV–visible region. DPA is likely to be adsorbed on Al_2O_3 and the DRS of DPA adsorbed Al_2O_3 shows low reflectance in the UV-A region. Fig. 7 displays the DRS of DPA-adsorbed Al_2O_3 and bare Al_2O_3. The DRS of pristine Al_2O_3 shows high reflectance. The DRS exhibit absorption of UV-A light by the DPA adsorbed Al_2O_3. This absorption is likely to result in electronic excitation of the adsorbed DPA. The excited electron may move to Al^{3+} resulting in $Ph_2NH^{\bullet+}$ radical cation-formation. The reduced form of Al^{3+} (*i.e.*, Al^{2+}) may lose an electron to the adsorbed molecular oxygen yielding superoxide radical ion ($O_2^{\bullet-}$). The reaction of the formed radical cation with superoxide radical ion may afford the product. The possibility of mediation of the reaction by SiO_2 present in the reaction vessel is ruled out as the organic transformation in the absence of Al_2O_3 was also carried out using the same reaction vessel under identical experimental conditions.

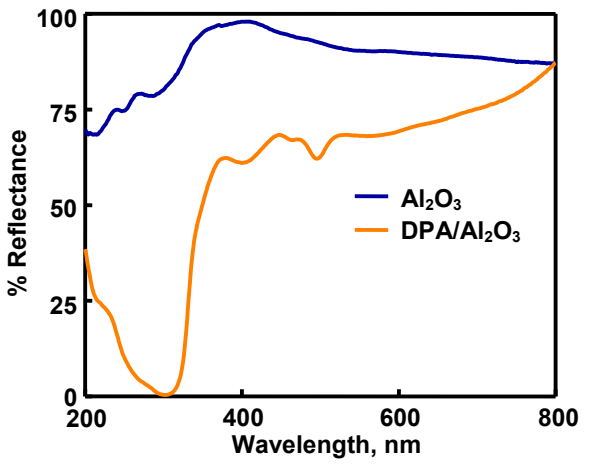

Fig. 7. The diffuse reflectance spectra.

3.4. Kinetics

The heterogeneous photoinduced reaction taking place in a continuously stirred tank reactor (CSTR) conforms to the kinetic law [16]:

rate of PBQ formation on Al_2O_3

$$= kK_1K_2SIC[\mathrm{DPA}]\gamma/(1 + K_1[\mathrm{DPA}])(1 + K_2\gamma)$$

where K_1 and K_2 are the adsorption coefficients of DPA and O_2 on illuminated Al_2O_3 surface, k is the specific rate of oxidation of DPA on Al_2O_3 surface, γ is the airflow rate, S is the specific surface area of Al_2O_3, C is the amount of Al_2O_3 suspended per liter and I is the light intensity. The data-fit to the Langmuir–Hinshelwood kinetic curve, drawn using a computer program, confirms the kinetic law (Figs. 2 and 4). The linear double reciprocal plots of surface reaction rate versus

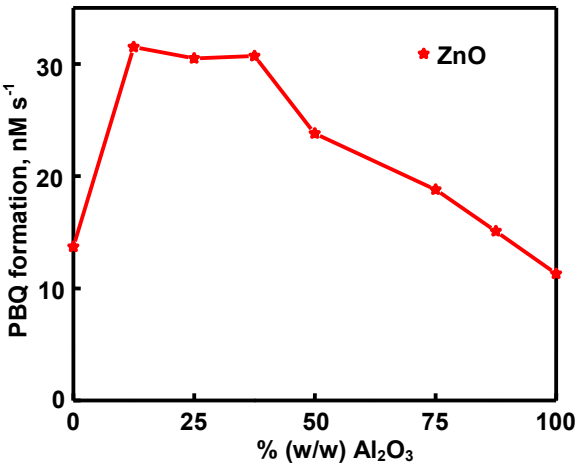

Fig. 8. Enhanced PBQ formation on mixing Al_2O_3 with ZnO; [DPA] = 5.0 mM, oxide-loading = 1.0 g, airflow rate = 7.8 mL s^{-1}, λ = 365 nm, I = 25.2 μE L^{-1} s^{-1}, illumination time = 30 min, volume of reaction solution = 25 mL.

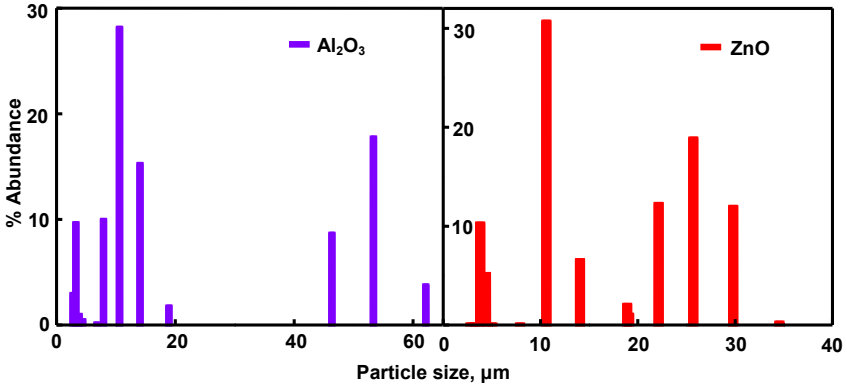

Fig. 9. Particles aggregation.

[DPA] and airflow rate also confirm the Langmuir–Hinshelwood kinetic law. The data-fit provides the adsorption coefficients K_1 and K_2 as 115 L mol^{-1} and 0.061 mL^{-1} s, respectively, and the specific reaction rate k as 18 μmol L m^{-2} $Einstein^{-1}$. However, the rate of PBQ formation on Al_2O_3 surface fails to increase linearly with Al_2O_3-loading. This is because of the high Al_2O_3 loading. At high Al_2O_3 loading, the surface area of the Al_2O_3 exposed to illumination does not correspond to the weight of Al_2O_3. The amount of Al_2O_3 used is beyond the critical amount corresponding to the volume of the reaction solution and reaction vessel; the whole quantity of Al_2O_3 is not exposed to light. The light-induced transformation lacks linear dependence on illumination intensity; less than first power dependence of surface-photoreaction rate on light intensity at high photon flux is well known [21].

3.5. Synergism by ZnO

Band gap-illumination of semiconductor mixture leads to vectorial transfer of photoformed electrons and holes from one semiconductor to another, which enhances the photocatalytic activity [22,23]. But what we observe here is enhanced phototransformation due to the presence of semiconductor ZnO nanoparticles with insulator Al_2O_3 nanoparticles. Fig. 8 presents the enhanced formation of PBQ with Al_2O_3 mixed with ZnO; the two nanoparticles are kept under suspension and at continuous motion by bubbling air through the illuminated solution. Aggregation of nanoparticles under suspension has been reported [24]. Fig. 9 presents the particle size distribution of Al_2O_3 and ZnO under suspension, determined by light scattering method. Examination of Fig. 9 along with the size of the particles obtained from XRD and BET methods reveals aggregation of the nanoparticles; under suspension, up to about 300 nanoparticles aggregate. As observed in individual Al_2O_3 and ZnO suspension, aggregation in the Al_2O_3–ZnO mixture under suspension is likely, and both Al_2O_3 and ZnO nanoparticles are likely to be present in the aggregate. This may lead to transfer of generated hole from the illuminated ZnO to the DPA molecule adsorbed on Al_2O_3 surface resulting in enhanced photooxidation. The densities and particle sizes of Al_2O_3 and ZnO are different and this may be a reason for not observing maximum enhanced photooxidation at 50% composition.

4. Conclusions

On the surface of Al_2O_3, DPA undergoes light-induced oxidative transformation to afford BPQ. The BPQ formation on Al_2O_3 increases with [DPA] and airflow rate and conforms to the Langmuir–Hinshelwood kinetic law. The PBQ formation on Al_2O_3 is large with UV-C light than with UV-A light. Al_2O_3 mixed with ZnO yields more PBQ than by the individual nanoparticles due to synergism.

Acknowledgment

Prof. C. Karunakaran is thankful to the Council of Scientific and Industrial Research (CSIR), New Delhi for the Emeritus Scientist Scheme [21(0887)/12/EMR-II].

References

[1] X. Lang, X. Chen, Zhao, Heterogeneous visible light photocatalysis for selective organic transformations, Chem. Soc. Rev. 43 (2014) 473–486.

[2] M.-Q. Yang, Y.-J. Xu, Selective photoredox using graphene-based composite photocatalysts, Phys. Chem. Chem. Phys. 15 (2013) 19102−19118.
[3] W. Feng, G. Wu, L. Li, N. Guan, Solvent-free selective photocatalytic oxidation of benzyl alcohol over modified-TiO_2, Green Chem. 13 (2011) 3265−3272.
[4] N. Zhang, S. Liu, X. Fu, Y.-J. Xu, Fabrication of coenocytic Pd@CdS nanocomposite as a visible light photocatalyst for selective transformation under mild conditions, J. Mater. Chem. 22 (2012) 5042−5052.
[5] G. Palmisano, E. Garcia-Lopez, G. Marci, V. Loddo, S. Yurdakal, V. Augugliaro, L. Palmisano, Advances in selective conversions by heterogeneous photocatalysis, Chem. Commun. 46 (2010) 7074−7089.
[6] Y. Shiraishi, T. Hirai, Selective organic transformations on titanium oxide-based photocatalysts, J. Photochem. Photobiol. C 9 (2008) 157−170.
[7] J. Literak, P. Klan, D. Heger, A. Loupy, Photochemistry of alkyl aryl ketones on alumina, silica-gel and water ice surfaces, J. Photochem. Photobiol. A 154 (2003) 155−159.
[8] J.T. Barbas, M.E. Sigman, A.C. Buchanan III, E.A. Chevis, Photolysis of substituted naphthalenes on SiO_2 and Al_2O_3, Photochem. Photobiol. 58 (1993) 155−158.
[9] T.A. Konovalova, A.M. Volodin, Photo-induced generation of radicals from *m*-dinitrobenzene adsorbed on γ-Al_2O_3: direct evidence for the formation of electron donor-acceptor (EDA) complexes with participation of solvent molecules, React. Kinet. Catal. Lett. 51 (1993) 227−232.
[10] S.F. Gerasimov, V.N. Filimonov, Photoinduced reactions of $H_2 + CO$ and $CH_4 + CO$ mixtures on η-Al_2O_3 and V/η-Al_2O_3, React. Kinet. Catal. Lett. 29 (1985) 387−393.
[11] M. Itou, A. Fujiwara, T. Uchino, Reversible photoinduced interconversion of color centers in α-Al_2O_3 prepared under vacuum, J. Phys. Chem. C 113 (2009) 20949−20957.
[12] A. Zanella, Control of apple superficial scald and ripening − a comparison between 1-methylcyclopropene and diphenylamine postharvest treatment, initial low oxygen stress and ultra low oxygen storage, Postharvest Biol. Technol. 27 (2003) 69−78.
[13] Y.C. Chang, P.W. Chang, C.M. Wang, Energetic probing for the electron transfer reactions sensitized by 9,10-dicyanoanthracene and 9-cyanoanthracene and their modified zeolite particle, J. Phys. Chem. B 107 (2003) 1628−1633.
[14] T.S. Lin, J. Retsky, ESR studies of photochemical reactions of diphenylamines, J. Phys. Chem. 90 (1986) 2687−2689.
[15] C. Karunakaran, S. Karuthapandian, Solar photooxidation of diphenylamine, Sol. Energy Mater. Sol. Cells 90 (2006) 1928−1935.
[16] C. Karunakaran, R. Dhanalakshmi, P. Gomathisankar, Photomineralization of phenol on Al_2O_3: synergistic photocatalysis by semiconductors, Res. Chem. Intermed. 36 (2010) 361−371.
[17] D.M. Adams, J.B. Raynor, Advanced Practical Inorganic Chemistry, John Wiley, New York, 1965.
[18] S. Puri, W.R. Bansal, K.S. Sidhu, Benzophenone-sensitized photooxidation of diphenylamine, Indian J. Chem. 11 (1973) 828.
[19] W.R. Bansal, N. Ram, K.S. Sidhu, Reaction of singlet oxygen: part I − oxidation of diphenylamine with singlet oxygen ($^1\Delta_g$) produced in situ, Indian J. Chem. B 14 (1976) 123−126.
[20] M.A. Fox, C.C. Chen, Mechanistic features of the semiconductor photocatalyzed olefin-to-carbonyl oxidative cleavage, J. Am. Chem. Soc. 103 (1981) 6757−6759.
[21] L. Vincze, T.J. Kemp, Light flux and light flux density dependence of the photomineralization rate of 2,4-dichlorophenol and chloroacetic acid in the presence of TiO_2, J. Photochem. Photobiol. A 87 (1995) 257−260.
[22] C. Karunakaran, R. Dhanalakshmi, P. Gomathisankar, Semiconductor-photocatalyzed degradation of carboxylic acids: enhancement by particulate semiconductor mixture, Int. J. Chem. Kinet. 41 (2009) 716−726.
[23] C. Karunakaran, R. Dhanalakshmi, P. Gomathisankar, G. Manikandan, Enhanced phenol-photodegradation by particulate semiconductor mixtures: interparticle electron-jump, J. Hazard. Mater 176 (2010) 799−806.
[24] M. Li, M.E. Noriega-Trevino, N. Nino-Martinez, C. Marambio-Jones, J. Wang, R. Damoiseause, F. Ruiz, E.M.V. Hock, Synergistic bactericidal activity of Ag-TiO_2 nanoparticles in both light and dark conditions, Environ. Sci. Technol. 45 (2011) 8989−8995.